ENGI3291: CFD Analysis using SolidWorks Coursework (Junya Ogawa)

Computational Fluid Dynamics (CFD) has many applications, such as in the areas of aeronautics, astronautics, various other engineering disciplines such as civil, process, chemical and environmental engineering [1] which makes it an extremely versatile and powerful tool in today's engineering sectors. However, CFD is also very dangerous: it is prone to be very volatile in terms of set-up, requiring specialised expertise to run, as well as taking up large amounts of processing time.

When using SolidWorks Flow Simulation, the following steps have to be taken [2]: Define all starting parameters on the Starting Wizard, defining boundary goals, the computational domain and the mesh, running the calculation and finally, creating cut plots/surface parameters depending on the objective of the simulation.

The main conservation laws used in SolidWorks Flow Simulation would be the mass, momentum and energy conservation laws, or more specifically, the Navier-Stokes Equations, with a Favre-Averaged Navier-Stokes formulation used for turbulent flows [2]. For the simulation to be well defined, initial known parameters such as the fluid velocities, pressures and temperature have to be defined [2]. Furthermore, fluid properties such as viscosity and density will have to be defined using the parameters and finally, the geometry of the flow domain has to be well-defined, in order to obtain well-defined results.

A mesh is used to generate a grid of data points within the flow domain where the aforementioned conservation laws can be calculated at [2]. In the case of SolidWorks, these equations are solved using an adaptation of the Finite Volume Method, where the control volumes are in the shape of rectangular parallelepipeds with orthogonal faces to the Cartesian coordinate system [2]. A goals and calculation monitor is used to ensure the specified values are converging instead of diverging, which ensured that the equation is solvable. It also has important information about any errors during calculation which may prove useful in troubleshooting.

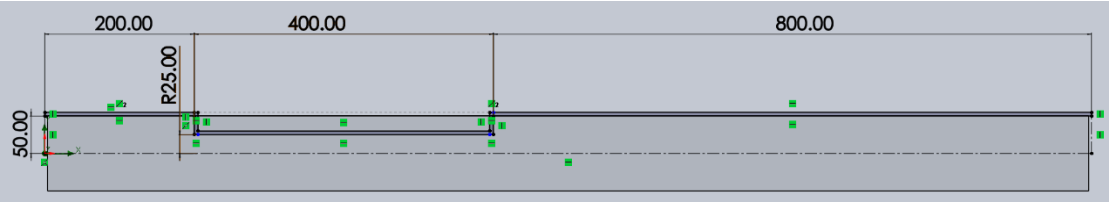

Figure 1: Dimensions of Pipe

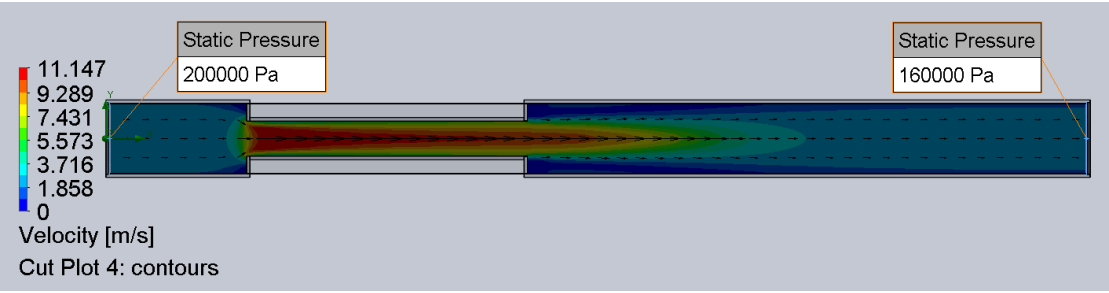

Figure 2: Velocity Contour Map of Pipe with Boundary Conditions

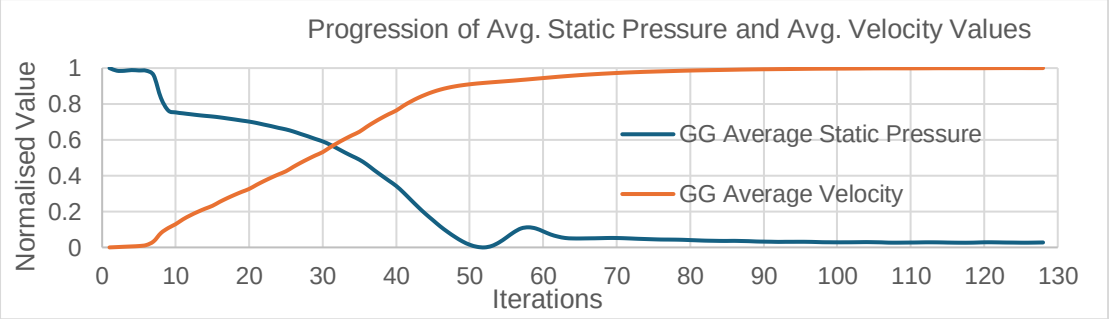

Figure 3: Goals and Convergence graph for GG values

Internal Pipe Flow Analysis

An analysis of a pipe flow with dimensions detailed in Figure 1, of thickness 5mm, roughness 0.0045mm and initial boundary conditions of $P_{inlet} = 2 \times 10^5$ Pa and $P_{outlet} = 1.6 \times 10^5$ Pa, with water flowing through at 50 degrees Celsius was conducted. The aim was to evaluate the backflow length percentage, the mass flow rate $\dot{m}$ and the static pressure at the end of the restrictor P_x using cut plots and surface parameters, the results of which are given below and in Figure 2 and compared to their theoretical counterparts where applicable.

To estimate the percentage of recirculation length, another velocity contour plot was created with 2 values, $-1\ \mathrm{ms}^{-1}$ and $1\ \mathrm{ms}^{-1}$. Using the measure tool, the length of recirculating flow was measured to be 0.261 m. As total length of the pipe 1.4 m, then the backflow length percentage is given as such:

$$\text{Backflow length percentage} = \frac{0.261}{1.4} \times 100\% = 18.6\%$$

The mass flow rate $\dot{m}$ was then obtained via obtaining the mass flow rate surface parameter on the inlet cap, with $\dot{m} = 15.31\ \mathrm{kg\ s}^{-1}$. Next, a lid was created and flow was ensured through the lid via the flow manager and using the pressure bulk average as a surface parameter to obtain $P_x = 0.149\ \mathrm{MPa}$. To theoretically validate the values of P and $\dot{m}$, the Steady State Flow Energy Equation (SFEE) was used, with, the following formulation, given that $z_{inlet} = z_{outlet} = 0$ and $u_{inlet} = u_{outlet}$ as they have the same diameter with $\dot{Q}$ being a constant throughout the pipe:

$$\frac{P_{inlet}}{\rho g} = \frac{P_{outlet}}{\rho g} + h_{L=0.2m} + h_{constrict} + h_{L=0.4} + h_{enlarge} + h_{L=0.8}$$

The total head loss across the pipe is then:

$$h_{total} = h_{L=0.2m} + h_{constrict} + h_{L=0.4} + h_{enlarge} + h_{L=0.8} = \frac{P_{start} - P_{end}}{\rho g}$$

Given the temperature of 50 degrees, $\rho = 988\ kgm^{-3}$ [3]. Thus,

$$h_{total} = \frac{2 \times 10^5 - 1.6 \times 10^5}{988 \times 9.81} = 4.127\ \mathrm{m}$$

Using a Moody diagram [4], the Fanning Friction Factors $f_{d=0.1m} \approx 0.0041$ and $f_{d=0.05m} \approx 0.0048$ were obtained respectively from the two k/d ratios and assuming full turbulent flow in the pipe. Via the head loss formulae for straight pipes [5], constrictors and enlargers [6]:

$$h_{total} \approx 13966\dot{V}^2 \Rightarrow \dot{V} = \sqrt{\frac{4.127}{13966}} \approx 0.01719\ \mathrm{m^3\ s^{-1}}$$

The Reynolds numbers for both diameters were calculated using the value given for $\dot{V}$ and the static viscosity $\mu = 5.465 \times 10^{-4}\mathrm{Pa\ s}$ [3]:

$$Re_{d=0.1m} = \frac{4\rho\dot{V}}{\pi d\mu} = \frac{(988)(4)(0.01719)}{\pi(0.1)(5.465 \times 10^{-4})} = 3.96 \times 10^5, Re_{d=0.05m} = \frac{(988)(4)(0.01719)}{\pi(0.05)(5.465 \times 10^{-4})} = 7.91 \times 10^5$$

Using the two Reynolds numbers, new values of the Fanning friction factors were calculated $(f_{d=0.1m} \approx 0.0044, f_{d=0.05m} \approx 0.0048)$ with the 2nd iteration of the volumetric flow rate $\dot{V}$ and Reynolds numbers Re:

$$\dot{V} \approx 0.0172\ \mathrm{m^3 s^{-1}}$$

$$\dot{m} = \rho\dot{V} = (988)(0.0172) \approx 16.99\ \mathrm{kg\ s^{-1}}$$

$$Re_{d=0.1m} = \frac{(988)(4)(0.0172)}{\pi(0.1)(5.465 \times 10^{-4})} = 3.96 \times 10^5, Re_{d=0.05m} = \frac{(988)(4)(0.0172)}{\pi(0.05)(5.465 \times 10^{-4})} = 7.91 \times 10^5$$

These yielded a similar value of the Fanning friction factors via the Moody diagram so the friction factors were at a sufficient accuracy. Comparing the two $\dot{m}$ values, the simulation yielded a value of $15.31\ \mathrm{m^3 s^{-1}}$ yet the theory yielded a value of $16.99\ \mathrm{m^3 s^{-1}}$, making the theoretical value about 89% accurate. This could be due to the SFEE being unable to factor in the actual length of straight pipe flow due to the flow regime between different sections changing gradually and not immediately in most cases, as well as the actual geometry of the pipe with sharp constrictions and enlargers. This affects the effective length variable in the Fanning equation. Furthermore, from these values it is noted that the flow regime throughout the pipe is meant to be turbulent as both Reynolds numbers are greater than 4000 [7], but water mostly flows in a

parabolic profile (Figure 2) and the only sources of eddies are before and after the restrictor due to the change in Reynolds number and the flow regime transitions between turbulence and high turbulence.

To determine the static pressure at the end of the restrictor, SFEE was again used with formulae for head losses:

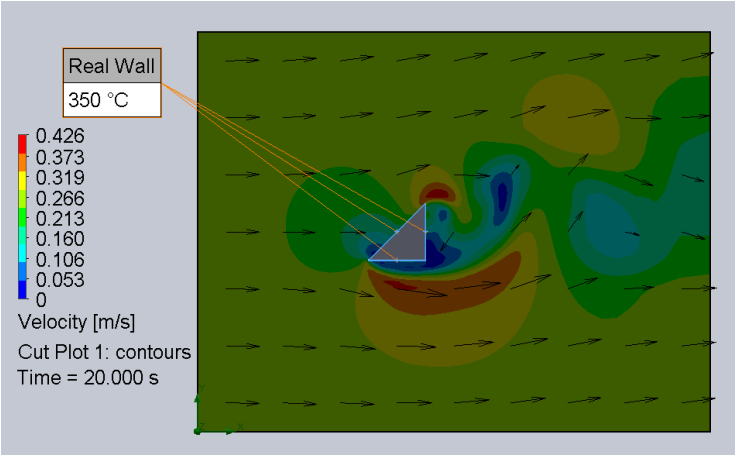

Figure 4: Vector contour map of coolant with boundary conditions

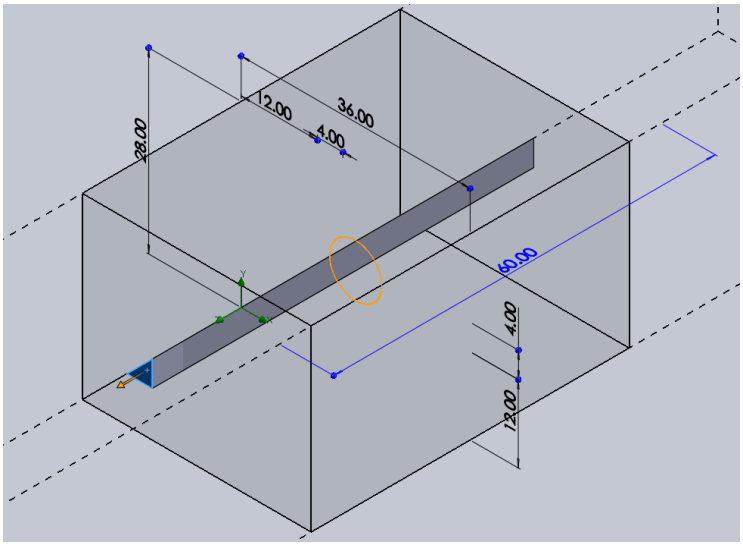

Figure 5: Isometric view of coolant with dimensions

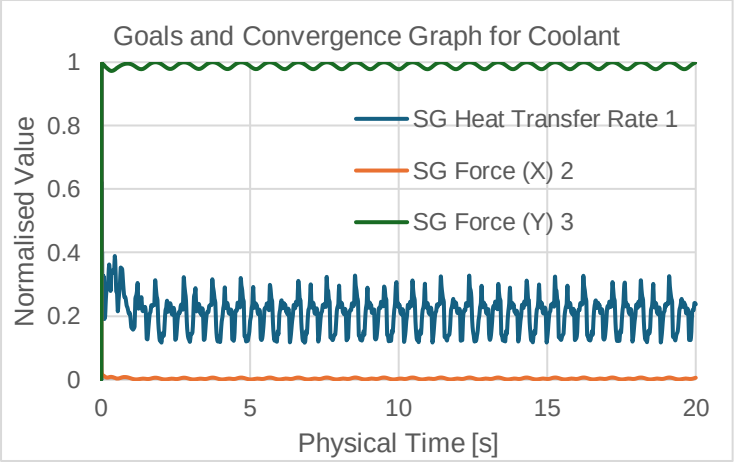

Figure 6: Goals and Convergence graphs for SG values for Coolant

$$\frac{P_{start}}{\rho g} + \frac{{u_{start}}^2}{2g} = \frac{P_x}{\rho g} + \frac{{u_x}^2}{2g} + h_{L=0.2} + h_{constrict} + h_{L=0.4}$$

$$\because u = \frac{4\dot{V}}{\pi d^2} \Rightarrow u^2 = \frac{16\dot{V}^2}{\pi^2 d^4}$$

$$\therefore P_x = 2 \times 10^5 + \frac{\rho}{2}\left(\frac{16\dot{V}^2}{\pi^2(0.1)^4} - \frac{16\dot{V}^2}{\pi^2(0.05)^4}\right) - \rho g(6420)\dot{V}^2$$

Substituting values of ρ and $\dot{V}$ found earlier:

$$P_x \approx 1.461 \times 10^5 \text{ Pa}$$

The simulation value of the static pressure at 1.49 bar is greater than that of the theoretical value at 1.46 bar, which makes the theoretical value 98% accurate and is not as drastic as that seen with the mass flow rate. However, there is still a small margin of error, and this could be due to factors such as water fluid resistance or the friction caused by the roughness of the pipe: even though it was accounted for in the Fanning formulae, the calculations of head losses remain an experimental estimate due to the highly unpredictable behaviour of high turbulence flows and will always differ from simulation.

External Coolant Rod Analysis

The coolant rod analysis was set-up with the computing domain at 50cm height with a 60cm long rod with a right-angled isosceles triangle cross-section. Carbon dioxide flowed through at a temperature of 150 degrees Celsius at 20 bars, and the simulation run for a physical time of 20 seconds.

Drag force was calculated via obtaining exporting the surface goals (for Force (X) and Force (Y)) to an Excel spreadsheet and obtaining the plot data. From there, the average value of the SG Force (X) value was used, from the physical time greater than 15s to 20s, and averaged said results using the AVERAGE function $F_D = 0.0302\text{N}$. To compare to theory, the drag coefficient C_D was calculated [8] using the drag force. As the gas used is carbon dioxide at 150 degrees Celsius at a pressure of 20 bar, the density was determined as $\rho = 25.77\ \text{kg m}^{-3}$ using a data table [3]. Thus, using the speed of air as 0.25 m/s and A as the area:

$$C_D = \frac{2F_D}{\rho U_m^2 A} = \frac{2(0.0302)}{(25.772)(0.25)^2(0.05 \times 0.4)} = 1.876$$

An Excel spreadsheet containing the values for the surface goal of the heat transfer rate was obtained, and the values from t = 15s to t = 20s was averaged using the AVERAGE function to get the heat transfer rate $\dot{Q} = 710$ W. For the rate of vortex shedding, it was the same as the frequency at which the Force (Y) values were oscillating at. Thus, via looking at the graph produced and the raw data, there were 5 complete oscillations between the time of t = 5.237 and t = 10.06. The period T of one oscillation is thus:

$$T = \frac{10.06 - 5.237}{5} = 0.965 \text{ s}$$

The formula for the Strouhal number [8] was used using the obtained period:

$$St = \frac{fL}{U_m} = \frac{\left(\frac{1}{0.965}\right) \times 0.04}{0.25} = 0.1658$$

Looking at similar shapes, experimental values of drag coefficient and Strouhal number of a cylinder with an isosceles right-angle triangle profile with apex angle facing the stream is 1.749 and 0.158 [8]. The Strouhal number and the drag coefficient were very accurate, with the Strouhal number being 95.3% accurate and the drag coefficient being 93.2% accurate. The source of inaccuracies could be from a few sources: firstly, being the air conditions: the simulation air was at 20 bar and 150 degrees Celsius, whilst the literature air was at room temperature and pressure, which meant that the simulation air had a greater density than literature. This would have made it harder to overcome inertial forces and thus have a greater drag coefficient in the simulation. Secondly, a reason why the Strouhal number could have been off was due to the orientation of the cylinder: the hypotenuse side of the cylinder in the literature was directly facing the stream, while in the simulation it was at 45 degrees. This re-orientation would have changed the geometry and the different vortex pattern, which changed the Strouhal number.

Bibliography

[1] J. Tu, G.-H. Yeoh, and C. Liu, ‘Introduction’, in *Computational Fluid Dynamics*, Elsevier, 2018, pp. 1–31. doi: 10.1016/B978-0-08-101127-0.00001-5.

[2] Dassault Systemes, *Technical Reference SolidWorks Flow Simulation 2022*. Dassault Systemes, 2022.

[3] E. W. Lemmon, I. H. Bell, M. L. Huber, and M. O. McLinden, ‘NIST Chemistry WebBook, NIST Standard Reference Database Number 69’, in *National Institute of Standards and Technology*, vol. 69, P. J. Linstrom and W. G. Mallard, Eds., Gaithersburg: National Institute of Standards and Technology. doi: https://doi.org/10.18434/T4D303.

[4] A. Bahadori, ‘Single-phase and Multiphase Flow in Natural Gas Production Systems’, in *Natural Gas Processing*, Elsevier, 2014, pp. 59–150. doi: 10.1016/B978-0-08-099971-5.00003-9.

[5] P. Thomas, ‘Steady-state compressible flow’, in *Simulation of Industrial Processes for Control Engineers*, Elsevier, 1999, pp. 50–59. doi: 10.1016/B978-075064161-6/50007-9.

[6] P. Kovarik, ‘Fluid Flow Theory’, in *Tutorial No. 1*, Ostrava: VSB, 2014.

[7] M. R. Islam and M. E. Hossain, ‘State-of-the-art of drilling’, in *Drilling Engineering*, Elsevier, 2021, pp. 17–178. doi: 10.1016/B978-0-12-820193-0.00002-2.

[8] N. Agrwal, S. Dutta, and B. K. Gandhi, ‘Experimental investigation of flow field behind triangular prisms at intermediate Reynolds number with different apex angles’, *Exp Therm Fluid Sci*, vol. 72, pp. 97–111, Apr. 2016, doi: 10.1016/j.expthermflusci.2015.10.032.